

Journal Pre-proofs

Interface Passivation and Electron Transport Improvement via Employing Calcium Fluoride for Polymer Solar Cells

Yuting Tang, Yu Pang, Xu Li, Beibei Zong, Bonan Kang, S. Ravi P. Silva, Geyu Lu

PII: S0021-9797(19)31485-7
DOI: <https://doi.org/10.1016/j.jcis.2019.12.025>
Reference: YJCIS 25765

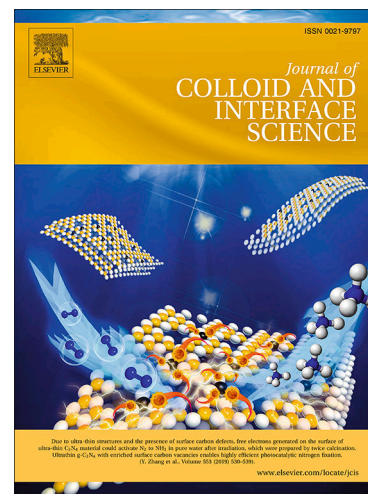
To appear in: *Journal of Colloid and Interface Science*

Received Date: 19 June 2019
Revised Date: 4 December 2019
Accepted Date: 6 December 2019

Please cite this article as: Y. Tang, Y. Pang, X. Li, B. Zong, B. Kang, S.R.P. Silva, G. Lu, Interface Passivation and Electron Transport Improvement via Employing Calcium Fluoride for Polymer Solar Cells, *Journal of Colloid and Interface Science* (2019), doi: <https://doi.org/10.1016/j.jcis.2019.12.025>

This is a PDF file of an article that has undergone enhancements after acceptance, such as the addition of a cover page and metadata, and formatting for readability, but it is not yet the definitive version of record. This version will undergo additional copyediting, typesetting and review before it is published in its final form, but we are providing this version to give early visibility of the article. Please note that, during the production process, errors may be discovered which could affect the content, and all legal disclaimers that apply to the journal pertain.

© 2019 Published by Elsevier Inc.



Interface Passivation and Electron Transport Improvement via Employing Calcium Fluoride for Polymer Solar Cells

Yuting Tang^a, Yu Pang^a, Xu Li^a, Beibei Zong^a, Bonan Kang^{a,}, S. Ravi P. Silva^b and Geyu Lu^a*

^a State Key Laboratory of Integrated Optoelectronics, College of Electronic Science and Engineering, Jilin University, 2699 Qianjin Street, Changchun 130012, China

^b Nanoelectronics Centre, Advanced Technology Institute, University of Surrey, Guildford, Surrey GU2 7XH, United Kingdom

*Corresponding author: Bonan Kang

Tel.: +86 431 85168270; Fax: +86 431 85168270.

E-mail address: kangbn@jlu.edu.cn

Abstract

To enhance the performance of inverted structure polymer solar cells (PSCs), interfacial engineering considered as an effective and straightforward method was employed. In this study, to overcome the surface traps and energy level mismatches of the electron transport layer, a means of interface passivation by evaporating an ultrathin CaF_2 layer above ZnO thin film as the electron transport layer was successfully adopted. We display that CaF_2 layer could passivate the surface traps of ZnO thin film and decrease the interfacial barrier between PC_{61}BM and ZnO, so that electron transfer efficiency is facilitated, the recombination of electrons and holes is inhibited at the contact interface, and the series resistance is reduced. After the introduction of the CaF_2 layer, the short-circuit current and the fill factor was greatly improved, also the power conversion efficiency (PCE) was increased from 3.21% of the reference device without the CaF_2 layer to 4.22% in the inverted PSCs based on P3HT: PC_{61}BM bulk heterojunction photoactive layer. These results could have special guiding significance for high-efficiency PSCs and also great potential for applications of photovoltaic devices in the future.

Keywords: Interface passivation, polymer solar cells, CaF_2 layer, surface traps, interfacial barrier.

1. Introduction

Polymer solar cells (PSCs) have aroused widespread attention in the past decades owing to their remarkable merits of mechanical flexible, light weight, low-cost solution processing and so on [1-4]. Whereas the short life span and dreadful stability of PSCs devices are yet grim issues that have given rise to its failure to better develop, hence one means of alleviating this challenge is the use of inverted device structure that shows higher stability to air environment [5-7]. Although currently, the application of photoactive materials plays a key role in the inverted PSCs, the modifications of the interface between the electrode and the photoactive layer are the key step to improve the stability of the cells [8]. N-type metal oxide semiconductors PSCs such as Titanium dioxide (TiO_2), Zinc Oxide (ZnO), Stannic oxide (SnO_2) are commonly used as electron transport layer (ETL) in the inverted PSCs [9-11].

As an ETL, there is growing attention in ZnO in inverted PSCs, due to its easy sol-gel fabrication in low-temperature processing, outstanding electron mobility, proper energy levels, excellent optical transparency [12-15]. The energy levels of Zinc Oxide are about 4.3 eV (conduction band minimum) and 7.8 eV (valence band maximum). This energy band position enables ZnO to play a key role in electron collection and hole blocking. Nevertheless, the surfaces of ZnO thin film has a host of major defects such as the surface traps and inferior compatibility with photoactive materials that account for unsatisfactory interface contact, resulting in comparatively more electron-hole recombination and larger series resistance, thus having an adverse impact on the cells performance [16-19]. To overcome these drawbacks of ZnO thin film, passivation treatment is carried out on the defect state of ZnO thin film like the doping of polymer or metal and surface modification to improve the photovoltaic performance. The doping of ZnO with metal or polymer, such as aluminum (Al) [20], gallium (Ga) [21], indium (In) [22], poly(ethylene oxide) [23], poly[(9,9-bis(3'-(N,N-dimethylamino)propyl)-2,7-fluorene)-alt-2,7-(9,9-dioctylfluorene)] [24], polyethylenimine [25] and polyvinylpyrrolidone [26], could significantly

improve the electrical and optical properties of these films, thereby enhancing devices performance of inverted PSCs. Additionally, there are also lots of surface modifications of ZnO thin film including ultraviolet immersion, self-assembled monolayer modification and conjugated polymer and ethanolamine surface modification and so on. These have been intensively applied to modifying the ZnO surface [27-33], which can boost the generation and extraction of charge, thus improving the photovoltaic performance.

In this study, Calcium fluoride (CaF_2) was introduced to modify ZnO ETL, which served as an electron transport layer in the inverted PSCs. Herein, a series of ultrathin CaF_2 layer with different thicknesses are thermally evaporated between active layer and ZnO layer to decrease the energy barrier and facilitate electron transport from the photoactive layer to ZnO ETL for the inverted PSCs based on poly(3-hexylthiophene):(6,6)-phenyl-C₆₁-butyric acid methylester (P3HT:PC₆₁BM), which does not only enhanced J_{sc} but also improved FF. Thus, in this study, after optimizing the thickness of CaF_2 , the PCE of the cell was significantly enhanced from 3.21% to 4.22% for the P3HT:PC₆₁BM-based PSCs. Consequently, this study reveals the influence of CaF_2 as valid interface modification materials for the inverted PSCs. This study expounds the use of CaF_2 to solve the problems of low-temperature preparation and complex synthesis process, an effective and simple method to improve the performance of the device. It may be a promising material for other optoelectronic devices, which is conducive for large-scale industrial production.

2. Experimental section

2.1. Materials

The poly (3-hexylthiophene) (P3HT) and (6, 6)-phenyl-C₆₁ butyric acid methylester (PC₆₁BM) were purchased from Metals (Nebraska). With an admixture of PC₆₁BM in a ratio of 1:1 w/w, P3HT is dissolved in 1, 2-dichlorobenzene (DCB) to obtain 17 mg/mL solution in the glove box. The sol-gel ZnO precursor solution was prepared

using the method in previous publications. Zinc acetate dihydrate (Alfa Aesar, 99%) and ethanolamine (Sigma Aldrich, 99.5%) were added to the ethanol (Sigma Aldrich) under vigorous stirring to make 0.2 mol/L solution at 60 °C. Calcium fluoride (CaF₂) purchased from TIC was used to modify the electron transport layer.

2.2. Fabrication of polymer solar cells

The FTO-coated glass substrates are rinsed with methylbenzene, acetone, deionized water and isopropyl alcohol in an ultrasonic bath for 20 min in sequence, and then blow-dried with N₂. Before being treated with O₂ plasma for 5 min, the FTO-coated glass substrates are dried in a drying furnace. The ZnO precursor solution is spin-coated on FTO at 4000 rpm for 40 s, and then heated for 2 h at 200 °C in an ambient atmosphere. Then, the CaF₂ layer is thermally evaporated on the top of the ZnO layer successively at a deposition rate of about 0.05 Å/s under a deposition pressure of 6.0×10^{-4} Pa. The thickness of the CaF₂ layer varies between 0.5 nm, 1 nm, 1.5 nm, and 2 nm. Thereafter, P3HT:PC₆₁BM is spin-coated on the CaF₂ layer at a speed of 800 rpm for 36 s and then annealed for 10 min at 120 °C in an N₂-filled glovebox. Finally, MoO₃ and Ag are thermally evaporated under a deposition vacuum of 6.0×10^{-4} Pa. The photoactive area, determined by the overlap of FTO and Ag, is about 0.05 cm².

2.3. Instrument and characterization

The current density-voltage (J-V) measurements were conducted by a Keithley 2400 source meter under the illumination of AM 1.5G 100 mW/cm² using a solar simulator (SAN-EI ELECTRIC). The surface roughness and morphologies of the ZnO and CaF₂ films are obtained by atomic force microscope (AFM) in tapping mode (Veeco Dimension 3100). The incident photon-to-current conversion efficiency (IPCE) spectra of all devices are measured by Crowntech QTest Station 1000 AD apparatus. The ultraviolet photoelectron spectroscopy (UPS) is performed on High-Resolution Ultraviolet Photoelectron Spectrometer (R3000). Photoluminescence (PL) spectrums

are gained by a HORIBA iHR550 monochromator. The ultraviolet-visible absorption spectrums and the transmittance spectrums are measured by means of Shimadzu UV-1700 system. The total measurements were made under atmospheric environments in the absence of encapsulation.

3. Results and discussion

To elucidate the function of CaF_2 layer on the inverted PSCs, with the configuration of $\text{FTO}/\text{ZnO}/\text{CaF}_2/\text{P3HT:PC}_{61}\text{BM}/\text{MoO}_3/\text{Ag}$, the devices are first employed as shown in Fig. 1a. Four different thick of 0.5 nm, 1 nm, 1.5 nm and 2 nm CaF_2 are investigated in this study. Additionally, the control devices of $\text{FTO}/\text{ZnO}/\text{P3HT:PC}_{61}\text{BM}/\text{MoO}_3/\text{Ag}$ structure is also made for comparison, as well as the chemical structures of the inverted polymer solar cell photoactive layer materials are introduced in Fig. 1b.

To determine the function of the CaF_2 layer on the inverted PSCs, the performance of the cells are optimized by altering CaF_2 thickness, and the photovoltaic characteristics of the cells are analyzed. The relevant J-V curves of the optimized devices with pristine ZnO and with different thickness of CaF_2 layer is illustrated in Fig. 2 under AM 1.5 G illumination. The detailed photovoltaic parameters of these cells are summarized in Table 1, including V_{oc} , J_{sc} , FF, R_s and PCE, and the corresponding thicknesses of CaF_2 layer for the optimized devices are 0.5 nm, 1 nm, 1.5 nm, and 2 nm, respectively. It was observed that the device prepared from the P3HT:PC₆₁BM blend without CaF_2 layer exhibits an unsatisfactory PCE of 3.21%, whereas compared to the control device, the champion performance of 4.22% for the device with 1.5 nm thick CaF_2 interlayer is gained, which obtain a 31% improvement. The V_{oc} of pristine ZnO and ZnO/ CaF_2 are 0.62 V and 0.63 V, severally, with almost no emerging change. It was observed that J_{sc} is significantly enhanced and FF presents a visible increase with ZnO/ CaF_2 . When the thickness of CaF_2 layer is 1.5 nm, the J_{sc} increases from 8.93 mA/cm² to 10.51 mA/cm², and the FF also increases from 57.60%

to 64.18% for the inverted PSCs without and with CaF₂ layer. The results show the improved PCE may be ascribed to the decreased interfacial recombination because of the filling of surface defects by CaF₂ layer, yielding to increased J_{sc} and FF. With the further increase of CaF₂ thickness, the thicker CaF₂ layer is seen as an insulator engendering lower J_{sc}, FF, FCE and higher serial resistance R_s of the inverted PSCs.

In order to further figure out the causation for the enhanced performances for the inverted PSCs, the absorption spectrum of the controlled devices with ZnO and the optimized devices with ZnO cladding 1.5 nm thicknesses of the CaF₂ layer are observed and shown in Figure 3a. After the ZnO ETL is modified by the CaF₂ layer, the improved absorption of ZnO/CaF₂/P3HT:PC₆₁BM at the 350 to 625 nm region may be attributed to decreased interface-optical-losses or optical interference. Furthermore, the optical absorption of the photoactive layer is a vital portion of the light-to-electrical conversion step in the inverted PSCs, so it is essential for ETL to have high transmittance. The optical transmittance spectra of ZnO and ZnO/CaF₂ are first measured, as shown in Fig. 3b. ZnO/CaF₂ films possessed a similar transmittance with the ZnO film, showing that the visible light is permitted to pierce through ZnO/CaF₂ films in a great measure and further utilized by the photoactive layer of P3HT:PC₆₁BM.

As is reported, the well-matched energy level can help to achieve splendid charge transport, reduce the energy dissipation in charge separation course, and then affect the performance of devices. To verify the effect of CaF₂ on ZnO thin film, the energy level of ZnO/CaF₂ thin film is measured by UPS. The binding energy at the cutoff region (E_{cutoff} of ZnO/CaF₂ thin films) and the valence band region (E_{onset} of ZnO/CaF₂ thin films) are found to be 17.81 and 4.44 eV, respectively, which are shown in Fig. 4a. The optical bandgap (E_g) could be determined from the under Tauc plot equation [34]:

$$(\alpha h\nu)^2 = A(h\nu - E_g) \quad (1)$$

where α is the extinction coefficient, $h\nu$ represents the incident photon energy, and A denotes a material constant. Thus, according to Tauc plot equation, we can obtain the band gap of ZnO/CaF₂ thin films. As shown in Fig. 4b, the E_g of ZnO/CaF₂ thin film

is 3.64 eV.

The valence band (VB) energy levels are determined by relying on the UPS data using the following equation [35]:

$$VB = hv - (E_{\text{cutoff}} - E_{\text{onset}}) \quad (2)$$

where hv represents the incident photon energy (with a He I of 21.22 eV). The VB of ZnO/CaF₂ is calculated to be -7.8 eV, and then the corresponding conduction band (CB) energy levels are estimated to be -4.2 eV in accordance with VB and bandgap of ZnO/CaF₂.

In our previous study, the CB of ZnO is -4.3 eV [34]. On the basis of the corresponding schematic energy level structure of the inverted cells, as depicted in Fig. 4c, the CB of the ZnO/CaF₂ thin films lies between the CB of ZnO (-4.3 eV) and the lowest unoccupied molecular orbital of PC₆₁BM (-3.9 eV). Based on the above investigations, the change of CB between ZnO and ZnO/CaF₂ showed that CaF₂ can pull down the CB of ZnO. As a result, the energy barrier is lowered at the interface of the ZnO thin film and PC₆₁BM layer, thus electrons could be effectively extracted from the photoactive layer and transferred from the photoactive layer to the ZnO thin film through a favorable path without giving rise to significant energy dissipation in this process. Therefore, it enhances the efficiency of charge collection, which will be conducive to the promotion in J_{sc} , which is in line with the data in Table 1.

The surface morphology has a notable effect on cells characteristics. Thus, the surface topography and roughness of CaF₂-modified ZnO are investigated by AFM using tapping-mode, and the results are presented in Fig. 5. With a scanning region of 5 $\mu\text{m} \times 5 \mu\text{m}$, the AFM height images indicate that the root-mean-square (RMS) roughness of 22.5 nm emerges from the ZnO on FTO. Nevertheless, after the introduction of CaF₂ on FTO/ZnO, it was observed that the surface roughness of FTO/ZnO/CaF₂, extracted from the AFM analysis, decreased from 22.5 nm to 20.2 nm. Thereby, the changes in surface topography and roughness mean that the CaF₂ layer may fill a portion of the grooves on the surface of the ZnO thin film. Furthermore, a smoother film has lesser defects, which is beneficial to diminish the probability of interface trap charge recombination and inhibit the leakage current, thus

improving the extraction of electrons. Moreover, the smooth surface of ZnO/CaF₂ could play an essential role in gaining good interface contact with the photoactive layer. As shown in Fig. 2, this result can be used to elucidate why inverted PSCs with ZnO/CaF₂ bilayer obtain higher J_{sc} and FF compared to the inverted PSCs with pristine ZnO ETL.

Fig. 6a shows the dark J-V characteristics of the inverted cells with and without CaF₂ layer. It was found that the inverted PSCs with CaF₂ layer, under forward and reverse bias voltage, exhibits better diode characteristics with a lesser leakage current, which enhances the diode rectifying ratios. The dark current promptly ascends at a low positive bias voltage, indicating an enhanced extraction of charge from the photoactive layer to ZnO thin film, which in turn reduces charge recombination, thus increasing J_{sc} and FF. In addition, the reduced dark current clarifies lower R_s , which can boost charge transport. Furthermore, to further certify the photocurrent enhancement, Fig. 6b compares the IPCE spectrums of the inverted cells with ZnO/CaF₂ layer and without CaF₂ layer, which suggests that improvements ranging from 350 to 700 nm. Moreover, the cells with CaF₂ layer at 535 nm exhibit a maximal IPCE value of 68% and the cells without CaF₂ at 540 nm show a lesser value of 57%, reflecting the enhanced photon utilization. The calculated J_{sc} are 8.37 mA·cm⁻² and 9.62 mA·cm⁻², respectively, which are in unanimity with the measured short-circuit current within a few percent. The main reasons for this increase may be ascribed to the promoted charge extraction and transport capability on account of the insertion of CaF₂, resulting in the enhancement of J_{sc} .

PL spectrums are further employed in investigating the charge transfer characteristics and recombination. It can be seen that ZnO/P3HT and ZnO/CaF₂/P3HT, as shown in Figure 7, exhibit PL emission intensity with double peaks at 655 nm and 710 nm, and this double peaks are generally ascribed to the photoluminescence emission from P3HT thin film [36]. The incident photons are absorbed by the P3HT thin film coupled with the ground-state electron and excited to a high energy state in this process. The excited electrons rapidly relax to the ground state, resulting in PL emission. It should be noted that the P3HT thin film with CaF₂

layer reveals weaker photoluminescence emission yields than without CaF_2 layer, indicating more effective photoelectron quenching resulting in extraction from the photoactive layer to electrode. These results show that the remarkable reduced photoluminescence intensity may be attributed to the more effective quenching of photoelectrons owing to reduced carrier recombination and the emergence of better electron transmission from the photoactive materials to electrode.

4. Conclusion

In summary, based on the preparation approaches of previous study [34,37], we have successfully introduced CaF_2 that acts as an outstanding interface modification layer by evaporation on the surface of ZnO thin film for boosting photovoltaic performance of the cells. The optimum thickness of CaF_2 for the P3HT:PC₆₁BM-based device was obtained, and the effect of CaF_2 in modifying the properties of ZnO ETL is systematically studied. AFM results reveal the smoother film surface of ZnO/ CaF_2 ETL is conducive to enhance interface contact with the photoactive layer. The low PL emission intensity of the ZnO/ CaF_2 /P3HT film indicates a better electron transport from the photoactive layer to the electrode. As a result, the PCE of the solar cell with 1.5nm- CaF_2 as the interface modification layer is 4.22%, giving rise to a 31.5% enhancement over the control device prepared without CaF_2 layer. It was found that the insertion of CaF_2 helps to passivate the surface of ZnO thin film, improves the optical absorption of the devices and decreases energy dissipation. It facilitates the transfer and collection of charge carriers. Researchers have introduced various methods of modifying ZnO thin films and have applied them to PSCs [27-32, 38-39]. Nevertheless, we employed evaporation of CaF_2 on ZnO thin film to avoid the problem of complex synthesis process. It is proved that evaporation of CaF_2 on ZnO thin film is an effective and simple method to improve surface morphology and enhance electron transport. The ZnO/ CaF_2 thin films could be regarded as an effective interface layer of PSCs. The findings reported here may be a

promising approach to enhance the performance of PSCs and other optoelectronic devices.

Acknowledgments

This research has been invested by the National Key Basic Research and Development Program of China (Grant No. 2016YFB0401001), Jilin Province Science and Technology Development Projects of International Cooperation (20190701015GH), Open Project of the State Key Laboratory of Supramolecular Structure and Materials of Jilin University (sklssm201809).

References

- [1] P. Shao, X. Chen, X. Guo, W. Zhang, F. Chang, Chen, Q. Liu, J. Li, Y Li, D. He, Facile embedding of SiO₂ nanoparticles in organic solar cells for performance improvement, *Organic Electronics* 50 (2017) 77-81.
- [2] Y. Dang, S. Shen, Y. Wang, X. Qu, S. Huang, Q. Dong, S.R.P. Silva, and B. Kang, Hole Extraction Enhancement for Efficient Polymer Solar Cells with Boronic Acid Functionalized Carbon Nanotubes doped Hole Transport Layers, *ACS Sustainable Chem. Eng.* 6 (2018) 5122-5131.
- [3] P. Zhang, X Xu, Y. Dang, S. Huang, X. Chen, B. Kang, S.R.P. Silva, PTFE/MoO₃ Anode Bilayer Buffer Layers for Improved Performance in PCDTBT:PC₇₁BM Blend Organic Solar Cells, *ACS Sustainable Chemistry & Engineering* 4 (2016) 6473-6479.
- [4] K. Borse, R. Sharma, H.P. Sagar, P.A. Reddy, D. Gupta, A. Yella, Efficient light trapping and interface engineering for performance enhancement in PTB7-Th: PC₇₀BM organic solar cells, *Organic Electronics* 41 (2017) 280-286.
- [5] Y. Şahin, S. Alem, R. Bettignies, J. Nunzi, Development of air stable polymer solar cells using an inverted gold on top anode structure, *Thin Solid Films* 476 (2005) 340-343.

- [6] Z. He, C. Zhong, S. Su, M. Xu, H. Wu, Y. Cao, Enhanced Power-Conversion Efficiency in Polymer Solar Cells Using an Inverted Device Structure, *Nat. Photonics*. 6 (2012) 591-595.
- [7] J. You, C.C. Chen, L. Dou, S. Murase, H.S. Duan, H.S. Hawks, T. Xu, H.J. Son, L. Yu, G. Li, Y. Yang, Metal Oxide Nanoparticles as an Electron-Transport Layer in High-Performance and Stable Inverted Polymer Solar Cells, *Adv. Mater.* 24 (2012) 5267-5272.
- [8] Z.Q. Liang, Q.F. Zhang, L. Jiang, G.Z. Cao, ZnO cathode buffer layers for inverted polymer solar cells, *Energy Environ Sci.* 8 (12) (2015) 3442-3476.
- [9] S. Li, Z. Li, C. Liu, X. Zhang, Z. Zhang, W. Guo, L. Shen, S. Ruan and L. Zhang, Interface passivation and electron transport improvement of polymer solar cells through embedding a polyfluorene layer, *Phys. Chem. Chem. Phys.* 19 (2017) 15207-15214.
- [10] Z.A. Tan, W.Q. Zhang, Z.G. Zhang, D.P. Qian, Y. Huang, J.H. Hou, Y.F. Li, High-performance inverted polymer solar cells with solution-processed titanium chelate as electron-collecting layer on ITO electrode, *Adv. Mater.* 24 (11) (2012) 1476-1481.
- [11] V.H. Tran, R.B. Ambade, S.B. Ambade, S.H. Lee, I.H. Lee, Low-Temperature Solution-Processed SnO₂ Nanoparticles as a Cathode Buffer Layer for Inverted Organic Solar Cells, *ACS Appl. Mater. Interfaces* 9 (2) (2017) 1645-1653.
- [12] L.K. Jagadamma, M. Abdelsamie, A.E. Labban, E. Aresu, G.O. Ngongang Ndjawa, D.H. Anjum, D. Cha, P.M. Beaujuge, A. Amassian, Efficient inverted bulk-heterojunction solar cells from low-temperature processing of amorphous ZnO buffer layers, *J. Mater. Chem. A* 2 (2014) 13321-13331.
- [13] M. Jorgensen, K. Norrman, S. A. Gevorgyan, T. Tromholt, B. Andreasen, F.C. Krebs, Stability of polymer solar cells. *Adv. Mater.* 24 (5) (2012) 580-612.
- [14] R. Po, C. Carbonera, A. Bernardi, N. Camaioni, The Role of Buffer Layers in Polymer Solar Cells, *Energy Environ. Sci.* 4 (2) (2011) 285-310.
- [15] Y. M. Sun, J.H. Seo, C.J. Takacs, J. Seifter, A.J. Heeger, Inverted polymer solar cells integrated with a low-temperature-annealed sol-gel-derived ZnO Film as an

- electron transport layer, *Adv. Mater.* 23 (14) (2011) 1679-1683.
- [16] A. Gadisa, Y. Liu, E. T. Samulski, R. Lopez, Minimizing interfacial losses in inverted organic solar cells comprising Al-doped ZnO, *Appl. Phys. Lett.* 100 (2012) 253903.
- [17] M. Hartel, S. Chen, B. Swerdlow, H.Y. Hsu, J. Manders, K. Schanze, F. So, Defect-induced loss mechanisms in polymer-inorganic planar heterojunction solar cells, *ACS Appl. Mater. Interfaces* 5 (2013) 7215-7218.
- [18] S. Bai, Y. Jin, X. Liang, Z. Ye, Z. Wu, B. Sun, Z. Ma, Z. Tang, J. Wang, U. Wurfel, F. Gao, F. Zhang, Ethanedithiol Treatment of Solution-Processed ZnO Thin Films: Controlling the Intragap States of Electron Transporting Interlayers for Efficient and Stable Inverted Organic Photovoltaics, *Adv. Energy Mater.* 5 (2015) 1401606.
- [19] Y. Liu, Y. Li, H. Zeng, ZnO-Based Transparent Conductive Thin Films: Doping, Performance, and Processing, *J. Nanomater.* 2013 (2013) 1-9.
- [20] T. Stubhan, I. Litzov, N. Li, M. Salinas, M. Steidl, G. Sauer, K. Forberich, G.J. Matt, M. Halik, C.J. Brabec, Overcoming interface losses in organic solar cells by applying low temperature, solution processed aluminum-doped zinc oxide electron extraction layers, *J. Mater. Chem. A* 1 (19) (2013) 6004-6009.
- [21] K.S. Shin, K.H. Lee, H.H. Lee, D. Choi, S.W. Kim, Enhanced Power Conversion Efficiency of Inverted Organic Solar Cells with a Ga-Doped ZnO Nanostructured Thin Film Prepared Using Aqueous Solution, *J. Phys. Chem. C* 114 (37) (2010) 15782-15785.
- [22] R. Biswal, A. Maldonado, J. Vega-Perez, D.R. Acosta, M. De La Luz Olvera, Indium Doped Zinc Oxide Thin Films Deposited by Ultrasonic Chemical Spray Technique, Starting from Zinc Acetylacetonate and Indium Chloride, *Materials* 7 (2014) 5038-5046.
- [23] S.Y. Shao, K.B. Zheng, T. Pullerits, F.L. Zhang, Enhanced performance of inverted polymer solar cells by using poly(ethylene oxide)-modified ZnO as an electron transport layer, *ACS Appl. Mater. Interfaces* 5 (2) (2013) 380-385.
- [24] N. Wu, Q. Luo, Z. Bao, J. Lin, Y. Li, C. Ma, Zinc oxide: Conjugated polymer

nanocomposite as cathode buffer layer for solution processed inverted organic solar cells, *Sol. Energy Mater. Sol. Cells* 141 (2015) 248-259.

[25] H.C. Chen, S.W. Lin, S.W. Jiang, Y.W. Su, K.H. Wei, Solution-processed zinc oxide/polyethylenimine nanocomposites as tunable electron transport layers for highly efficient bulk heterojunction polymer solar cells, *ACS Appl. Mater. Interfaces* 7 (11) (2015) 6273-6281.

[26] C.E. Small, S. Chen, J. Subbiah, C.M. Amb, S.W. Tsang, T.H. Lai, J.R. Reynolds, F. So, High-efficiency inverted dithienogermole–thienopyrrolodione-based polymer solar cells, *Nat. Photonics* 6 (2) (2011) 115-120.

[27] S. Bai, Y. Jin, X. Liang, Z. Ye, Z. Wu, B. Sun, Z. Ma, Z. Tang, J. Wang, U. Würfel, F. Gao, F. Zhang, Ethanedithiol Treatment of Solution-Processed ZnO Thin Films: Controlling the Intragap States of Electron Transporting Interlayers for Efficient and Stable Inverted Organic Photovoltaic, *Adv. Energy Mater.* 5 (2015) 1401606.

[28] S.B. Dkhil, D. Duché, M. Gaceur, A.K. Thakur, F.B. Aboura, L. Escoubas, J.J. Simon, A. Guerrero, J. Bisquert, G. GarciaBelmonte, Q. Bao, M. Fahlman, C. Videlot-Ackermann, O. Margeat, J. Ackermann, Interplay of Optical, Morphological, and Electronic Effects of ZnO Optical Spacers in Highly Efficient Polymer Solar Cells, *Adv. Energy Mater.* 4 (2014) 1400805.

[29] S. Woo, W. Hyun Kim, H. Kim, Y. Yi, H.-K. Lyu, Y. Kim, 8.9% Single-Stack Inverted Polymer Solar Cells with Electron-Rich Polymer Nanolayer-Modified Inorganic Electron-Collecting Buffer Layers, *Adv. Energy Mater.* 4 (2014) 1301692.

[30] B.A. MacLeod, B.J. Tremolet de Villers, P. Schulz, P.F. Ndione, H. Kim, A.J. Giordano, K. Zhu, S.R. Marder, S. Graham, J.J. Berry, A. Kahn, D.C. Olson, Stability of inverted organic solar cells with ZnO contact layers deposited from precursor solutions, *Energy Environ. Sci.* 8 (2015) 592-601.

[31] Q. Bao, X. Liu, Y. Xia, F. Gao, L.-D. Kauffmann, O. Margeat, J. Ackermann, M. Fahlman, Effects of ultraviolet soaking on surface electronic structures of solution processed ZnO nanoparticle films in polymer solar cells, *J. Mater. Chem. A* 2 (2014) 17676-17682.

- [32] L. Nian, W. Zhang, N. Zhu, L. Liu, Z. Xie, H. Wu, F. Wurthner, Y. Ma, Photoconductive Cathode Interlayer for Highly Efficient Inverted Polymer Solar Cells, *J. Am. Chem. Soc.* 137 (2015) 6995-6998.
- [33] S.K. Hau, Y.J. Cheng, H.L. Yip, Y. Zhang, H. Ma, A.K.Y. Jen, Effect of Chemical Modification of Fullerene-Based Self-Assembled Monolayers on the Performance of Inverted Polymer Solar Cells, *ACS Appl. Mater. Interfaces* 2 (2010) 1892-1902.
- [34] S. Huang, Y. Tang, A. Yu, Y. Wang, S. Shen, B. Kang, S.R.P. Silvab, G. Lu. Solution-processed SnO₂ nanoparticle interfacial layers for efficient electron transport in ZnO-based polymer solar cells. *Organic Electronics* 62 (2018) 373-381.
- [35] J. Meyer, S. Hamwi, M. Kroger, W. Kowalsky, T. Riedl, A. Kahn, Transition metal oxides for organic electronics: energetics, device physics and applications, *Adv. Mater.* 24 (40) (2012) 5408-5427.
- [36] H. Wang, H.Y. Wang, B.R. Gao, L. Wang, Z.Y. Yang, X.B. Du, Q.D. Chen, J.F. Song, H.B. Sun, Exciton diffusion and charge transfer dynamics in nano phase-separated P3HT/PCBM blend films, *Nanoscale* 3 (5) (2011) 2280-2285.
- [37] D. C. Lim, W. H. Shim, K. Kim, H. O. Seo, J. Lim, Y. Jeong, Y. D. Kim, K. H. Lee, Spontaneous formation of nanoripples on the surface of ZnO thin films as hole-blocking layer of inverted organic solar cells, *Solar Energy Materials & Solar Cells* 95 (2011) 3036-3040.
- [38] T. Yang, M. Wang, C. Duan, X. Hu, L. Huang, J. Peng, F. Huang and X. Gong, Inverted polymer solar cells with 8.4% efficiency by conjugated polyelectrolyte, *Energy Environ. Sci.* 5 (2012) 8208-8214.
- [39] X. Cai, T. Yuan, X. Liu, and G. Tu, Self-Assembly of 1-Pyrenemethanol on ZnO Surface toward Combined Cathode Buffer Layers for Inverted Polymer Solar Cells, *ACS Appl. Mater. Interfaces* 9 (2017) 36082-36089.

All figure captions:

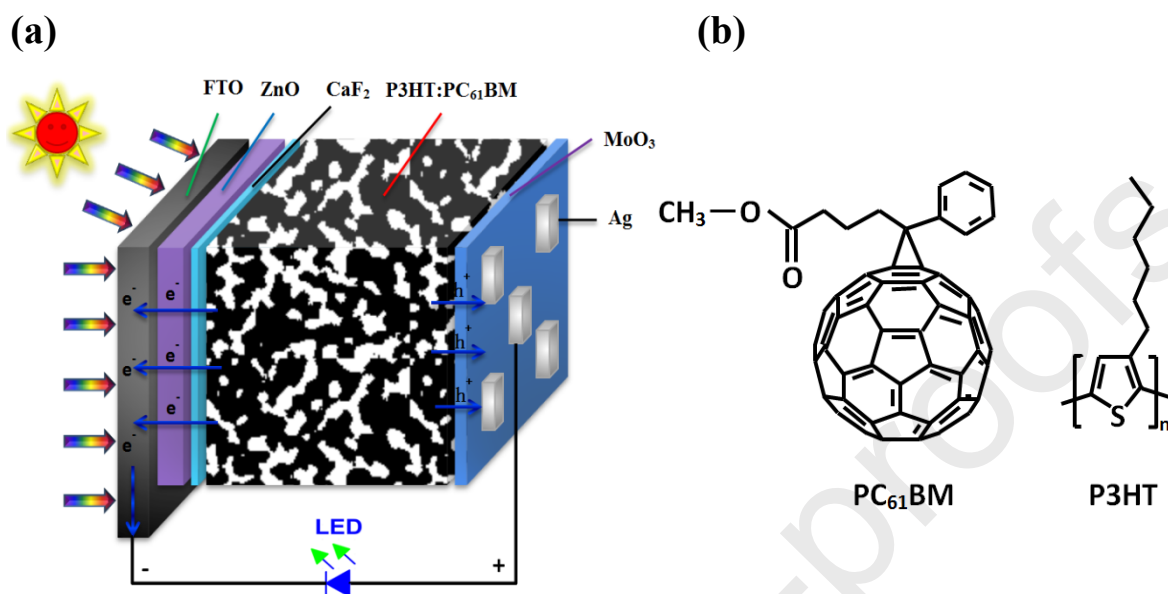


Fig. 1. (a) The schematic of the inverted solar cell architecture in this work. (b) The chemical structures of active layer materials.

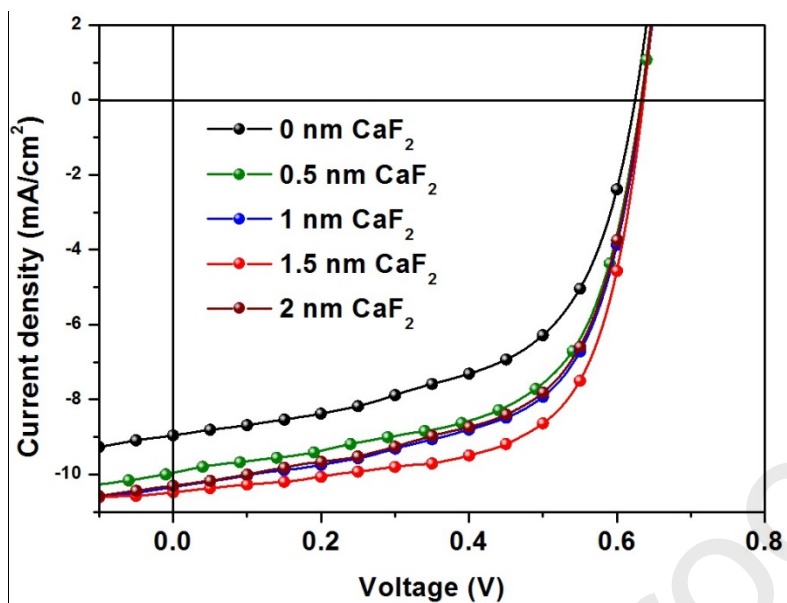


Fig. 2. The J-V curves characteristics of all the devices with pristine ZnO and with different the thickness of CaF₂ interlayer.

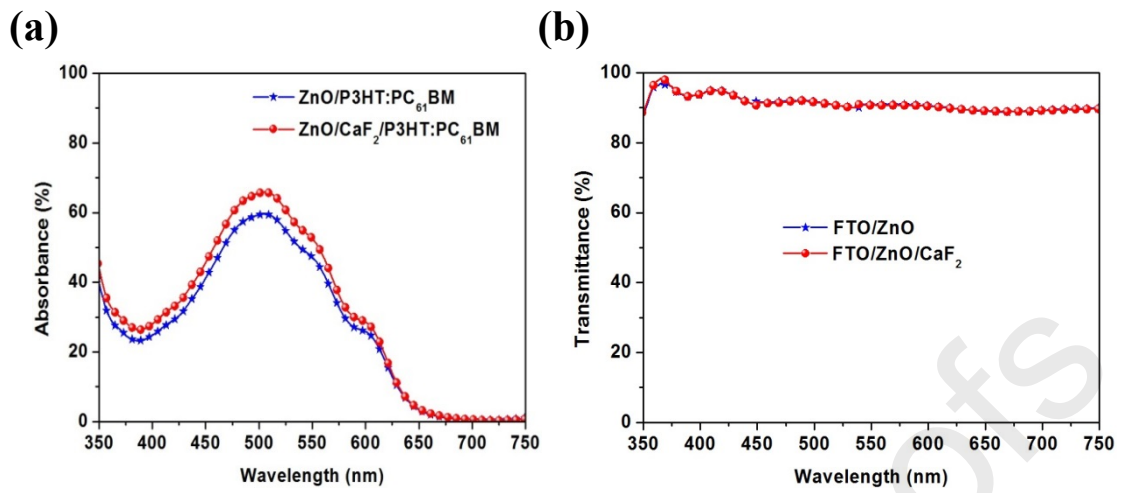


Fig. 3. (a) The absorption spectra of ZnO/P3HT:PC₆₁BM and ZnO/CaF₂/P3HT:PC₆₁BM. (b) Optical transmission spectra of ZnO and ZnO/CaF₂.

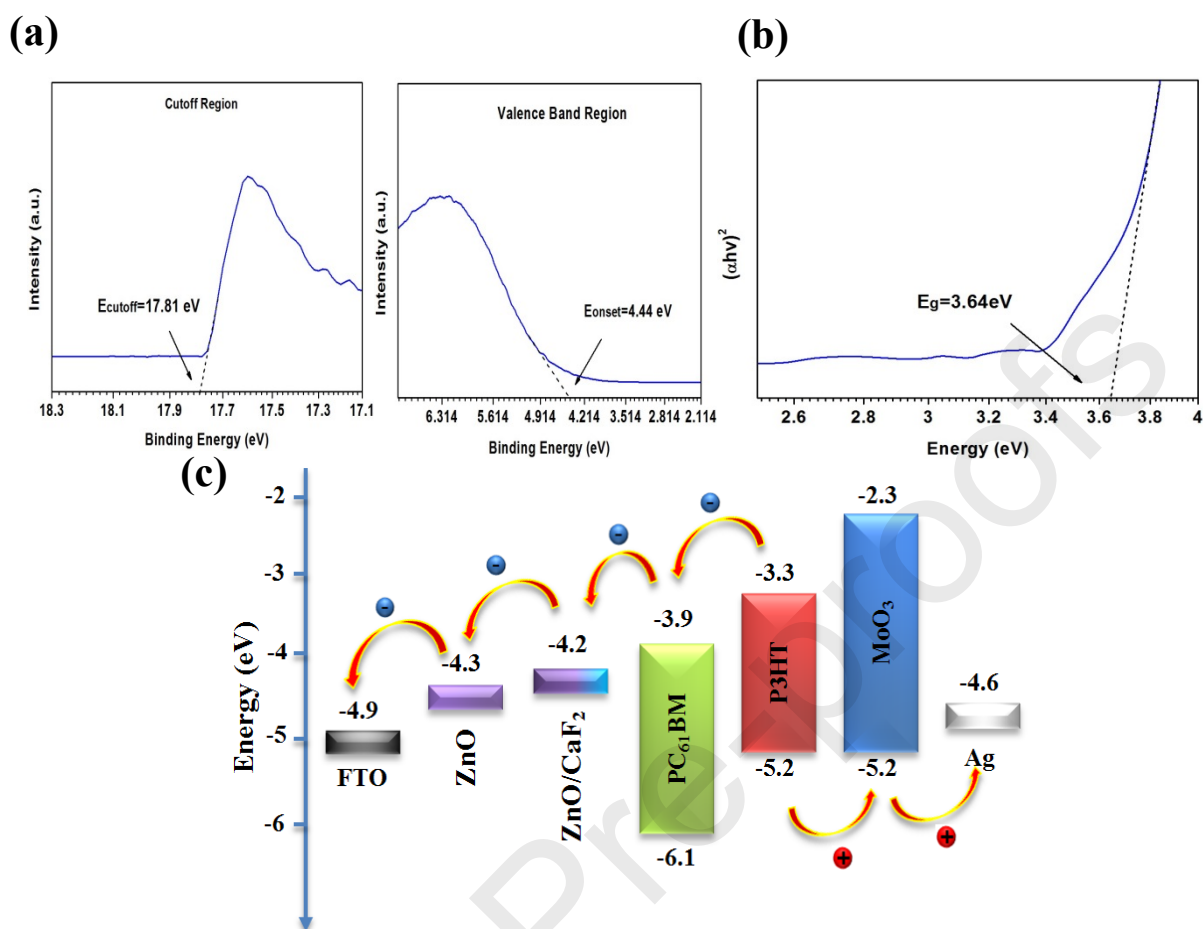


Fig. 4. UPS results of (a) cutoff region and valence band region for ZnO/CaF₂ bilayer thin films.

(b) Tauc plot for ZnO/CaF₂ thin films. (c) Energy band structure diagram of the inverted PSCs.

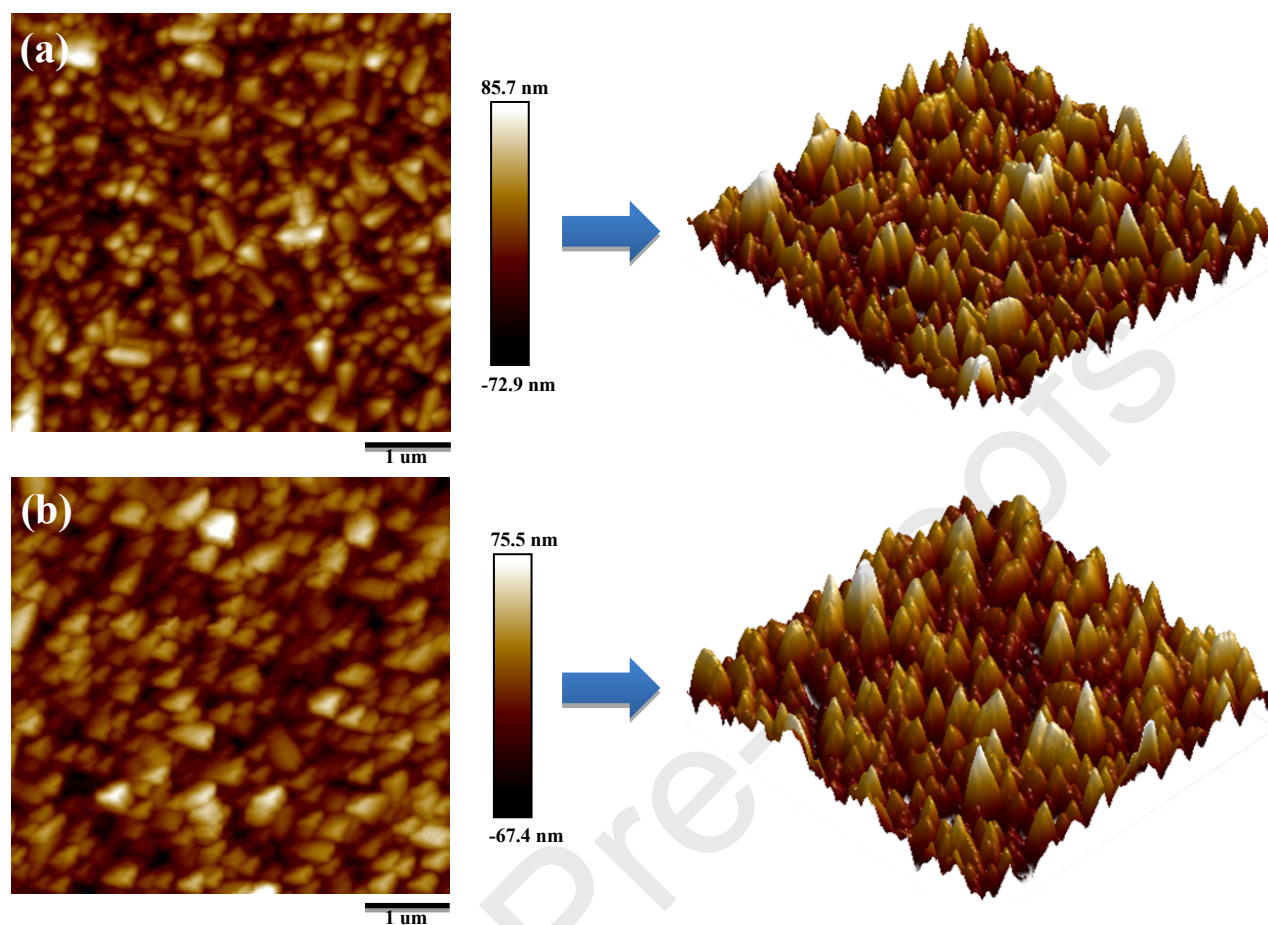


Fig. 5. AFM height images (5 $\mu\text{m} \times 5 \mu\text{m}$) of (a) pristine ZnO and (b) ZnO/CaF₂ bilayer thin films on top of an FTO/glass substrate.

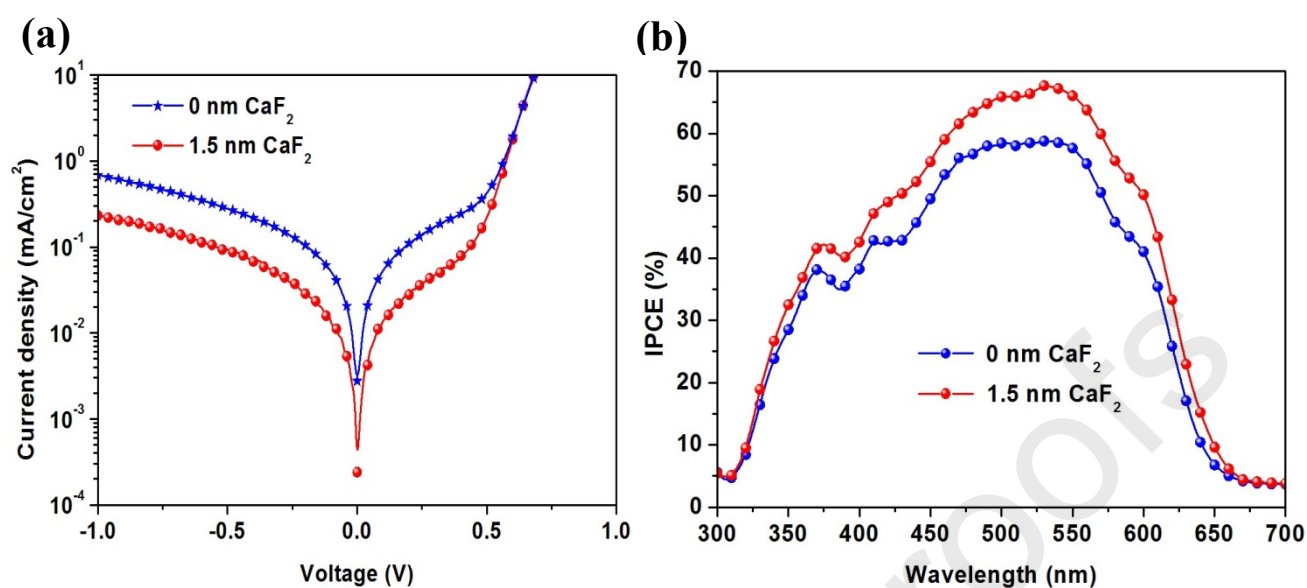


Fig. 6. (a) the dark J-V characteristics of the inverted PSCs. (b) The IPCE spectrums of the inverted PSCs with and without CaF₂ layer under 100 mW/cm² AM 1.5 G illumination.

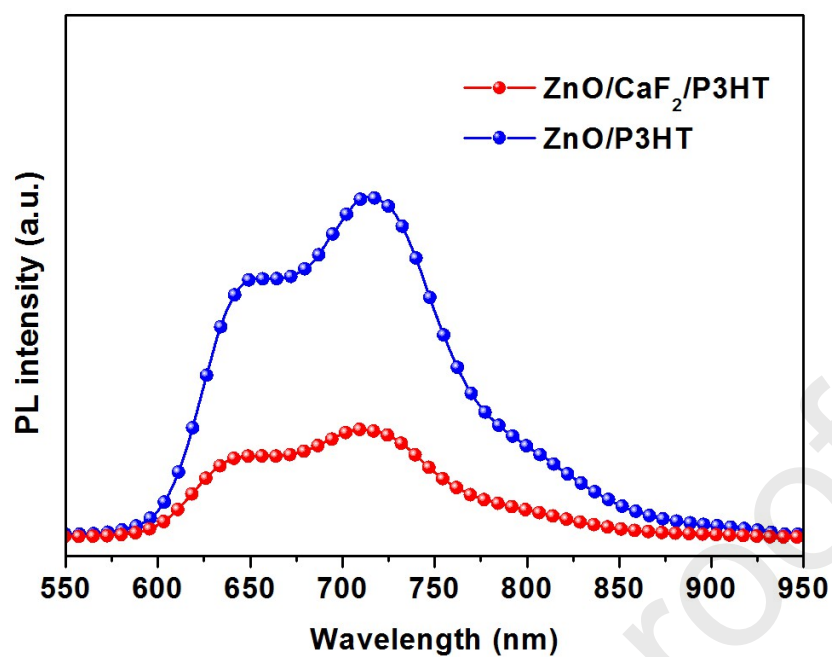


Fig. 7. PL spectrums of ZnO/P3HT thin films and ZnO/CaF₂/P3HT thin films.

All tables:**Table 1**

Photovoltaic parameters of all devices

ZnO/x nm-CaF ₂	V _{oc} (V)	J _{sc} (mA·cm ⁻²)	FF (%)	PCE (%)	R _s (Ω·cm ²)
x=0	0.61±0.01	8.93±0.03	57.60±0.02	3.21±0.03	7.71
x=0.5	0.63±0.02	10.18±0.03	59.20±0.02	3.81±0.03	5.82
x=1	0.63±0.02	10.36±0.03	61.49±0.02	4.04±0.02	5.31
x=1.5	0.63±0.02	10.51±0.03	64.18±0.02	4.22±0.03	5.18
x=2	0.63±0.02	10.27±0.03	61.88±0.02	4.02±0.01	5.53

Author Contributions Section

Yuting Tang: Conceptualization, Methodology, Investigation, Writing-Original Draft.

Yu Pang: Data Curation, Validation.

Xu Li: Data Curation.

Beibei Zong: Data Curation.

Bonan Kang: Resources, Supervision, Project administration, Funding acquisition.

S. Ravi P. Silva: Supervision.

Geyu Lua: Supervision.

Declaration of interests

☒ The authors declare that they have no known competing financial interests or personal relationships that could have appeared to influence the work reported in this paper.

☐ The authors declare the following financial interests/personal relationships which may be considered as potential competing interests:

Graphical abstract

